

Intracellular pH (pHi) Measurements in the *In Vitro* Tadpole Brainstem: Direct Correlations between Changes in pHi and Ventilation

Debora A. Zamora¹, C.R. Marutha Ravindran¹, James N. Bayne¹, James C. Leiter² and Matthew J. Gdovin^{1,*}

¹Department of Biology, The University of Texas at San Antonio, 1 UTSA Circle, San Antonio, TX 78249, USA

²Department of Physiology, Dartmouth Medical School, HB 7700, Hanover NH 03755, Germany

Abstract: Central respiratory chemoreceptors measure pH in the brain stem and are an integral part of the neural circuitry that modulates respiratory rhythmogenesis, specifically in response to hypercapnic acidosis. Central respiratory chemoreceptor membrane potential and/or action potential firing rate are altered in response to changes in intracellular pH (pHi), which changes with the hydration of CO₂ in both the extracellular and intracellular space, however the role of cellular changes in chemoreceptor properties on respiratory motor output has been difficult to identify. We studied whole nerve respiratory activity while simultaneously visualizing pHi dynamics using the pH-sensitive dye, BCECF, in the spontaneously active *in vitro* tadpole brainstem. The isolated, superfused tadpole brainstem is well oxygenated and retains synaptic connectivity among respiratory central pattern generators, central respiratory chemoreceptors, and respiratory motor neurons under physiological conditions, where mammalian preparations do not. An ammonium prepulse was used to selectively induce a decrease in pHi. Our results show intracellular pH is regulated differently in cells located in chemosensitive and non-chemosensitive regions of the tadpole brainstem during hypercapnia. We were also able to show an inverse correlation between pHi in cells located in chemosensitive regions of the tadpole brainstem and whole nerve respiratory-related activity. Using this approach, the microenvironment of individual cells may be manipulated while monitoring real time changes in pHi, neuronal activity and ventilatory-related activity to elucidate the role of a variety of signals in eliciting changes in ventilation.

Keywords: Central respiratory chemoreceptors, respiration, carbon dioxide, pH.

INTRODUCTION

The characterization of the cellular mechanisms involved in CO₂/H⁺ chemoreception has been the focus of recent research [1,2]. Unequivocally identifying a chemosensitive cell as being respiratory in nature continues to be problematic when studying central respiratory chemoreception. It is difficult to establish firm causal relationships between stimulus, effector elements and responses in intact preparations because each neuron makes only a small contribution to the overall response – different patterns of neuronal activity can only be correlated with particular responses. In reduced preparations, causal links may be established between sequential neural elements, but the biological importance of any particular response is moot since the neural activities are frequently unconnected to meaningful physiological responses. Brain areas involved in respiratory chemosensitivity have been identified by the discrete application of CO₂/H⁺ [3,4,5] and differences in rates of pHi regulation between putative chemosensitive and non-chemosensitive cells have

been proposed [6]. In addition, separate studies using pH-sensitive dyes and whole cell recordings have found significant correlations between pHi and neuronal firing rate [1]. Moreover, lesion studies in which particular classes of neurons are killed, knocked out or inhibited have identified particular neuronal populations in specific regions of the brain that contribute to CO₂ chemosensitivity, but these studies do not reveal the positive functional aspects of these neurons (i.e., how does the neuronal activity of these neurons mediate chemosensitivity) since the neurons of interest are absent from the animal or preparation [7-9]. While these studies provide valuable information regarding the cellular effects of CO₂/H⁺ and the neuronal populations responsible for central CO₂ chemosensitivity, it has not been possible to attribute changes in respiratory motor output to the specific pattern of neuronal activity during changes in CO₂ or pH in specific neurons. Addressing this issue requires simultaneous measurements of pHi dynamics and whole nerve respiratory output in a single preparation. The development of the *in vitro* tadpole brainstem preparation and simultaneous measurement of pHi using 2',7'-bis-(2-carboxyethyl)-5-(and-6)-carboxyfluorescein, acetoxymethyl ester (BCECF, AM) provides a novel model to determine if there is a relationship between changes in pHi in specific cells and neural activity related to ventilation.

*Address correspondence to this author at the Department of Biology, The University of Texas at San Antonio, 1 UTSA Circle, San Antonio, Texas 78249, USA; Tel: 210-458-4275; Fax: 210-458-5658; E-mail: matthew.gdovin@utsa.edu

Here we describe a method to simultaneously measure pHi dynamics in small numbers of neurons located in known chemosensitive brainstem regions and whole nerve activity related to the respiratory output in a reduced amphibian preparation, the *in vitro* tadpole brainstem of the larval *Lithobates catesbeianus*, formerly *Rana catesbeiana*. Recent development of neonatal and adult rodent *in vitro*, *en bloc*, and *in situ* preparations have provided valuable information regarding the neural substrates of respiratory rhythmogenesis [10-15]. Concerns regarding the interpretation of use of these preparations are valid and have been reported [14,16]. One concern centers around the “respiratory-like” motor pattern recorded from these preparations, as they do not produce the augmenting inspiratory and declining post-inspiratory patterns recorded *in vivo* [14], but instead demonstrate a rapid onset burst pattern similar to gasping [17]. In addition, these preparations are conducted in conditions that do not mimic physiological conditions *in vivo*; supraphysiological bath K⁺ and reductions in bath temperature as low as 25°C produce a preparation with a hypoxic, hyperkalemic, acidic core [18-19]. Attempting to use these preparations to study central respiratory chemoreception is limited, as “metabolic conditions such as hypercapnia and hypoxia in the deeper brainstem tissue may impair network connectivity and synaptic function, resulting in either a 2- or 1 phase pattern” rather than the 3-phase rhythm associated with eupnea [20]. Smith *et al.*, [20] reported a switch from the eupnic 3-phase pattern to a 1 phase pattern in response to changes in CO₂ in the *in situ* perfused rat brainstem-spinal cord preparation. The tadpole brainstem of *Lithobates catesbeianus* is well oxygenated [21], retains the circuitry necessary to produce spontaneous respiratory output and has a measurable respiratory response to changes in CO₂ [22-23]. For these reasons, the ability to monitor whole nerve respiratory activity and changes in pHi simultaneously provides a powerful tool to dissect the mechanistic connections among the neural elements involved in respiratory responses to CO₂.

METHODS

In Vitro Brainstem Preparation

Animals

Experiments were performed on *Lithobates catesbeianus* tadpoles (BCECF calibration n = 57; Hypercapnic Acidosis n = 55) of developmental stages 3-20 [24] of either sex obtained from a commercial supplier (Sullivan, TN USA). All tadpoles were housed in aquaria and were maintained at 24 – 26°C with a 12h:12h light:dark photoperiod. Tadpoles were fed on a daily basis (Fish Flakes, Wardly) as needed so that food was not a limiting resource. Animal care and experimental protocols were approved by the University of Texas at San Antonio Institutional Animal Care and Use Committee.

Dissection

Tadpoles were anesthetized in 3-aminobenzoic acid ethyl ester (MS 222; Sigma-Aldrich, St. Louis, MO) dissolved in distilled water (1:10,000) until unresponsive to tail pinch and weighed. Using a dissecting microscope, the dorsal cranium was removed, and the cranial and spinal nerves were severed at their ostia. After the dura and arachnoid were removed

dorsally and ventrally, the brainstem was transected just caudal to the level of the second spinal (hypoglossal) nerve root and just rostral to cranial nerve V. Throughout the dissection, the brainstem was continuously superfused with artificial cerebrospinal fluid (aCSF) bubbled with O₂. The composition of the aCSF was as follows (in mM): NaCl 104; KCl 4.0; MgCl₂ 1.4; D-glucose 10; NaHCO₃ 25; and CaCl₂ 2.4. Following dissection, the brainstem was incubated in oxygenated 2',7'-bis-(2-carboxyethyl)-5-(and-6)-carboxy-fluorescein, acetoxymethyl ester (BCECF-AM; Molecular Probes, Eugene, Oregon).

Recording Chamber

The brainstem was removed as described above then transferred to a superfusion recording chamber maintained at room temperature, 21-23 °C. The brainstem was secured ventral side up to the floor of the chamber using a stainless steel anchor with Lycra® threads 0.1 mm thick and 2.0 mm apart (SHD-26GKIT, Warner Instrument Corporation). The bottom of the chamber was constructed from a 22 x 40 mm glass cover slip with a thickness of 0.13-0.17mm and had a working volume of 180 µl. The brainstem was superfused with aCSF that had been equilibrated with a CO₂/O₂ gas mixture in an external tonometer at room temperature. The superfusate entered the recording chamber through an inflow aperture at a rate of 2 ml/min and exited from the opposite end *via* a vacuum. The aCSF pH was measured in the tonometer (Orion, 420A) and bath (Orion 9863BN), and aCSF pH was adjusted by changing the amount of CO₂ bubbling into the tonometer.

Whole Nerve Recordings

Neural recordings of fictive gill and lung ventilation were obtained from the roots of CN VII using glass suction electrodes. Suction electrodes were made from thin walled borosilicate glass capillaries (O.D. 1 mm; ID 0.5 mm), pulled to a fine tip with a horizontal micropipette puller (Flaming/Brown, P-97). Pipettes were cut with a diamond pen and smoothed by heating on an open flame to achieve inner tip diameters that fit the cranial nerve of interest (approximately 220 to 315 µm). A 0.25 mm diameter silver grounding wire was wrapped around the outside of the pipette down to the tip of the electrode. Suction electrodes were filled with filtered aCSF solution described above. Efferent neural activity was amplified (10,000X; AM Systems, 1700), filtered (10 Hz to 500 Hz), simultaneously averaged with a moving time averager (CWE, MA-821) and digitized and recorded on a Pentium 4 PC (Datapac 2000 software).

Fluorescence Imaging

BCECF is a dual excitation ratio metric dye that when excited at 440 nm (its iso-excitation point) is pH insensitive and when excited at 495 nm is pH-sensitive [25]. BCECF reports only cytoplasmic changes in pH and allows rapid kinetic changes of pH as small as 0.01 to be monitored [26-28.] The addition of acetoxymethyl (-AM) makes BCECF temporarily membrane permeable and therefore provides a non-invasive methods of dye loading [26-28.] Once inside the cell, hydrolysis of the acetyl ester linkage by enzymatic cleavage regenerates the less permeable original compound [26]. BCECF has a slow rate of dye leakage and does not appear to be harmful to cells [26].

Dye Preparation

BCECF-AM stock 0.004 M (Molecular probes, Eugene, OR) was made by dissolving 1 mg BCECF-AM in methylsulfoxide (DMSO) (201 μ L). Fifty μ L of each BCECF stock solution was added to 10 ml aCSF for a final BCECF concentration of 40 μ M.

Dye Incubation

The *in vitro* tadpole brainstem was incubated in 10 ml of 40 μ M BCECF, prepared as described above, for 30 minutes in the dark. Following dye incubation, the brainstem was washed for 30 minutes in oxygenated aCSF.

Imaging of BCECF-loaded Neurons

The superfusion chamber containing the brainstem was placed under an upright microscope (ECLIPSE E600FN Nikon, Melville, NY) mounted with a charge-coupled device (CCD) camera (MicroMAX, Roper Scientific, Trenton, NJ) connected to a Pentium computer (Hewlett Packard Company, Palo Alto, CA). Neurons were excited for 200 – 400 msec with light from a 175-W xenon arc lamp (Sutter Instrument, Novato, CA) that was filtered to 495 or 440 nm using a high speed filter changer (Lambda DG-4, Sutter Instrument, Novato, CA). Emitted light passed through a dichroic mirror with a high pass cut off of 515 nm and a 535 \pm 25 nm emission filter (Chroma Technology, Brattleboro, VT). Data were collected with an image acquisition software program (MetaMorph/MetaFluor, Universal Imaging Corporation, Downingtown, PA) for later analysis.

BCECF Calibration

The calibration solution contained in (mM): KCl 104; CaCl₂ 2.4; MgCl₂ 1.4; N-methyl-D-glucamine (NMDG)-N-2-hydroxyethylpiperazine-N'-2-ethanesulfonic acid (HEPES); D-glucose 10; Sucrose 25; and 0.016 nigericin titrated with either KOH or HCl to desired pH. All calibration points were normalized to pH 7.2 and a calibration curve ranging from pH 6.2 to 8.6 was constructed.

One-Point Nigericin Technique

Brainstems from subsequent experiments were superfused with high K⁺/nigericin solution set at pH 7.2 at the end of each experiment. Once fluorescence acquisitions reached steady state an averaged nigericin response was acquired to normalize experimental fluorescence ratios (495/440). Normalized fluorescence was converted into pHi values using the equation obtained from the above mentioned calibration curve.

Hypercapnic Acidosis

Intracellular (n=55) emitted BCECF fluorescence during normocapnic (bath pH = 7.8) and hypercapnic (bath pH = 7.4) bath conditions was recorded in cells located in chemosensitive and non-chemosensitive regions of the spontaneously rhythmic *in vitro* tadpole brainstem preparation. Briefly, the brainstem was dissected and incubated in BCECF (40 μ M) for 30 minutes as described above. Following the 30 minute aCSF wash, the brainstem was transferred to a superfusion chamber (RC-26GLP, Warner Instrument Corporation) for optical recordings of intracellular fluorescence. The superfusate was equilibrated in external tonome-

ters with an O₂/CO₂ gas mixture to desired pH values and had a flow rate of 2 ml/min. The brainstem was superfused with control aCSF (pH7.8) for at least 10 minutes and baseline fluorescence was acquired. The PCO₂ was then raised to attain a pH value of 7.4 and after a 10 minute equilibration period, fluorescence acquisitions were taken every minute for 10 minutes. Baseline fluorescence (pH 7.8) post hypercapnic exposure was attained and after a 10 minute equilibration period acquisitions were taken every minute for 10 minutes.

A subset of animals of developmental stages 3-10 (n = 10) and 11-20 (n= 8) were used to describe developmental changes in respiratory activity during hypercapnic acidosis, while simultaneously collecting optical recordings of pHi. Respiratory variables, mentioned above in *Respiratory Variables*, were acquired and analyzed using Datapac 2000 software. Experimental time included five experimental conditions: control (C1), transition to hypercapnic acidosis (T1), hypercapnic acidosis (HA), transition back to control (T2), and final control (C2). Gill and lung activity were analyzed separately. For statistical analyses, data were normalized to a percent change from the initial control (C1) value.

Statistical Analysis

Since each animal experienced all five experimental periods, Repeated Measure (RM) One-way ANOVAs were run for each respiratory variable measured. If data did not meet the assumptions of parametric statistical tests, then a non-parametric RM Mann-Whitney Rank Sum Test was used. *P* values <0.05 were considered significant. Unless otherwise stated, values reported are mean \pm one standard error of the mean (SEM).

pHi Regulation in Chemosensitive and Non-chemosensitive Regions

pHi regulation of cells in chemosensitive (n = 35) and non-chemosensitive (n = 22) regions of the tadpole brainstem was determined using the fluorescence dye, BCECF. Briefly, BCECF loaded cells were exposed to hypercapnic acidosis and fluorescence acquisition were acquired every 15 seconds for the initial 5 minutes of hypercapnic exposure followed by acquisitions every 30 seconds for an additional 10 minutes. To determine if pHi regulation occurred, linear regressions were done from the lowest pHi value observed during hypercapnic acidosis to the average baseline hypercapnic response, the last 5 minutes of hypercapnic exposure.

Ammonia prepulse was used (n = 4) to determine if cells that lacked pHi regulation during hypercapnic acidosis were able to exhibit regulation during intracellular acidification at a constant pHo. Briefly, BCECF fluorescence was obtained in cells that were exposed to hypercapnic acidosis pH 7.4 and control solution pH 7.8. The brainstem was then superfused with NH₄Cl until the characteristic alkalization plateau was reached and started to decline, approximately 2 minutes. Upon exposure and removal of NH₄Cl, fluorescence acquisitions were taken every 15 seconds to monitor the changes in intracellular pH.

Statistical Analysis

A t-test was run to compare pHi regulation rates from cells located in chemosensitive and non-chemosensitive re-

gions of the tadpole brainstem. A t-test was run to compare pHi regulation rates during two different methods of intracellular acidification, hypercapnic acidosis and NH_4Cl prepulse. A t-test was run to compare levels of intracellular acidification during hypercapnic acidosis and NH_4Cl .

RESULTS

pHi Regulation in Chemosensitive and Non-chemosensitive Regions

The rate of pHi regulation during hypercapnic acidosis was significantly ($P < 0.05$) greater in cells located in non-chemosensitive regions ($n = 22$; 0.06 ± 0.14 pH unit change min^{-1}) than cells located in chemosensitive regions ($n = 34$; 0.01 ± 0.01 pH unit change min^{-1}) (Fig. 1). With respect to the presence of pHi regulation, there was a mixed population of cells within both non-chemosensitive and chemosensitive regions of the brainstem in that not all cells demonstrated pHi regulation. However, a larger percentage of cells within the non-chemosensitive region (76%) exhibited pHi regulation during hypercapnic acidosis compared to cells within chemosensitive regions (47%).

To determine if cells that lacked pHi regulation during hypercapnic acidosis exhibited the ability to regulate intracellular pH, a subset of cells ($n = 4$) from a chemosensitive region that did not exhibit pHi regulation during hypercapnic acidosis, were exposed to an ammonia prepulse (60 mM NH_4Cl was added to the perfusion bath for five minutes), an experimental treatment that causes an initial alkalosis followed by plateau alkalization as NH_4^+ enters the cells (probably through potassium channels), but causes a decrease in pHi at a constant pHo when NH_4Cl is removed from the perfusate and the intracellular NH_4^+ sheds a proton and leaves the cell as NH_3 . Although there was a similar drop in pHi during hypercapnic acidosis and the ammonia prepulse, the rate of pHi regulation was significantly ($P < 0.05$) greater following the ammonia prepulse induced intracellular acidification (0.015 ± 0.003 pH unit change min^{-1}) than during intracellular acidification associated with hypercapnic acidosis (0.003 ± 0.002 pH unit change min^{-1}). An example of the pHi profile recorded from a single cell located in a chemosensitive region exposed to an ammonia prepulse is shown in Fig. (2).

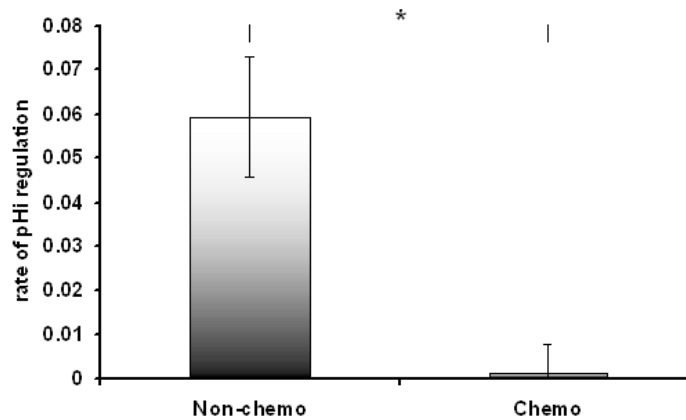


Fig. (1). pHi regulation in non-chemosensitive ($n = 22$) and chemosensitive ($n = 34$) regions of the tadpole brainstem during hypercapnic acidosis. pHi regulation (pH unit change min^{-1}) of cells located in non-chemosensitive regions (0.06 ± 0.14) was significantly* ($P < 0.05$) greater than pHi regulation of cells located in chemosensitive regions (0.01 ± 0.01).

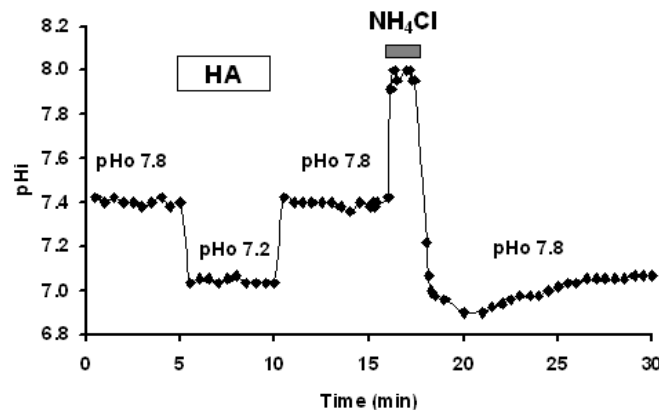


Fig. (2). pHi profile of a chemosensitive cell during control pH, hypercapnic acidosis, return to control, and NH_4Cl prepulse. Note that there is no pHi regulation following hypercapnic acidosis, but the same cell regulates pHi following intracellular acidification with NH_4Cl prepulse.

Correlation of pHi and Whole Nerve Respiratory Activity

Whole Nerve Activity

To describe the relationship between whole nerve respiratory activity during the transition to higher levels of CO₂ and pHi of cells located in documented chemosensory and non-chemosensory regions, we recorded respiratory activity from cranial nerve VII in tadpoles at Taylor and Kollros [24] developmental stages 3-10 (n = 10) and 11-20 (n = 8). Two distinct, developmentally-dependent respiratory patterns are observed *in vivo* [29] and may be recorded from respiratory-related cranial nerves *in vitro*: a relatively high frequency, low amplitude pattern corresponding to gill ventilation, and a low frequency, high amplitude pattern corresponding to lung ventilation [30-32]. To characterize the hypercapnic respiratory response, we measured both the lung burst frequency, cycle length, burst duration, inter-burst interval (IBI), and the amplitude of rectified, integrated nerve activity and the gill burst frequency, cycle length, burst duration, inter-burst interval (IBI), and amplitude. Experimental recording time included five experimental periods: control (C1), transition to hypercapnic acidosis (T1), hypercapnic acidosis (HA), transition back to control (T2), and final control (C2).

Gill Respiratory Variables – Early Developmental Stages

All preparations exhibited the expected high frequency, small amplitude fictive gill bursting pattern. In early stage developmental tadpoles, the gill respiratory values during superfusion with control aCSF were (in seconds): cycle time 1.54 ± 0.23 , burst duration 1.15 ± 0.10 , and IBI 0.39 ± 0.18 . There were no significant differences in gill burst frequency, cycle (Fig. 3), duration, and IBI in response to the exposure to hypercapnic acidosis in the early stage (Table 1). Gill burst amplitude measured in arbitrary units (au) did not change significantly throughout the different experimental conditions.

Gill Respiratory Variables – Late Developmental Stages

Late developmental stage tadpole brainstem preparations also exhibited the high-frequency, low-amplitude gill burst motor pattern (Table 1). Gill burst frequency (min^{-1}) in the late developmental stage preparations was not significantly altered by the experimental conditions. The gill burst cycle in the late developmental stage tadpoles during the transition to hypercapnia (1.90 ± 0.36) was not significantly different from control (1.84 ± 0.34); however significant gill cycle responses were observed during hypercapnia (HA), the transition to control (T2), and the final control condition (C2). In

Table 1. Gill and Lung Burst Frequency (min^{-1}), Cycle (sec), Duration (sec), Interburst Interval (IBI; sec), and Amplitude (au) Measured During Control (C1 & C2), Transition to (T1) and from (T2) Hypercapnic Acidosis (HA); in Early (Stages 6-10) and Late (Stages 11-20) Developmental Stage Tadpoles.

| | C1 | T1 | HA | T2 | C2 |
|---------------------|------------------|---------------------------|-------------------------|---------------------------|-------------------------|
| Gill - Early | | | | | |
| Frequency | 43.36 ± 3.91 | 43.84 ± 4.61 | 42.78 ± 4.16 | 45.15 ± 4.43 | 45.62 ± 4.11 |
| Cycle | 1.54 ± 0.23 | 1.58 ± 0.23 | 1.57 ± 0.19 | 1.51 ± 0.23 | 1.44 ± 0.17 |
| Duration | 1.15 ± 0.10 | 1.18 ± 0.21 | 1.17 ± 0.12 | 1.09 ± 0.12 | 1.10 ± 0.11 |
| IBI | 0.39 ± 0.18 | 0.41 ± 0.17 | 0.38 ± 0.12 | 0.43 ± 0.16 | 0.34 ± 0.11 |
| Amplitude | 0.17 ± 0.02 | 0.19 ± 0.02 | 0.18 ± 0.02 | 0.20 ± 0.03 | 0.18 ± 0.02 |
| Gill - Late | | | | | |
| Frequency | 39.22 ± 5.59 | 39.42 ± 5.66 | 34.60 ± 5.59 | 35.51 ± 5.59 | 38.80 ± 4.91 |
| Cycle | 1.84 ± 0.34 | 1.90 ± 0.36 | $2.22 \pm 0.46^\dagger$ | $2.09 \pm 0.38^\dagger$ | $1.72 \pm 0.24^\dagger$ |
| Duration | 1.21 ± 0.14 | 1.25 ± 0.14 | 1.25 ± 0.14 | $1.43 \pm 0.20^\dagger$ | $1.28 \pm 0.13^\dagger$ |
| IBI | 0.58 ± 0.22 | $0.65 \pm 0.25^\dagger$ | $0.79 \pm 0.29^\dagger$ | $0.65 \pm 0.25^\dagger$ | 0.45 ± 0.14 |
| Amplitude | 0.14 ± 0.02 | 0.15 ± 0.02 | 0.15 ± 0.02 | 0.14 ± 0.02 | 0.15 ± 0.02 |
| Lung - Late | | | | | |
| Frequency | 0.29 ± 0.12 | $1.06 \pm 0.30^\dagger$ | 0.96 ± 0.37 | 0.94 ± 0.25 | 0.63 ± 0.26 |
| Cycle | 8.15 ± 5.39 | $79.97 \pm 25.88^\dagger$ | 28.61 ± 13.32 | $60.62 \pm 31.80^\dagger$ | 34.81 ± 14.99 |
| Duration | 0.57 ± 0.19 | $1.21 \pm 0.12^\dagger$ | 0.79 ± 0.14 | $1.19 \pm 0.12^\dagger$ | 0.79 ± 0.17 |
| IBI | 7.79 ± 5.30 | $78.86 \pm 25.83^\dagger$ | 28.03 ± 13.19 | 59.64 ± 31.82 | 34.21 ± 14.93 |
| Amplitude | 0.19 ± 0.07 | $0.45 \pm 0.05^\dagger$ | 0.31 ± 0.05 | $0.50 \pm 0.05^\dagger$ | 0.36 ± 0.08 |

[†]Indicates a Significantly Different Percent Change from Control (C1).

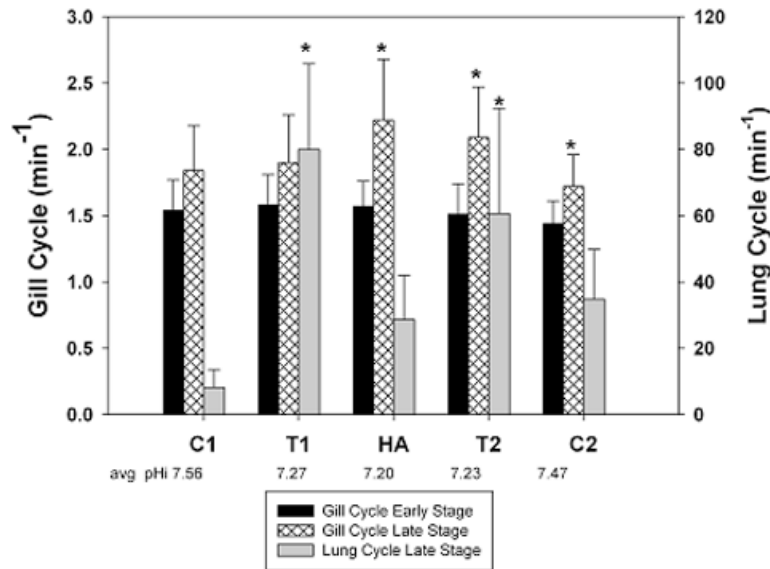


Fig. (3). Gill and lung burst cycle (min^{-1}) during control (C1), the transition to hypercapnia (T1), hypercapnic acidosis (HA), the transition from hypercapnia (T2) back to control bath pH (C2) for early and late developmental stage tadpoles. The average pHi in each of the five experimental conditions appears below each condition (* indicates significantly different from C1).

addition, gill burst duration during the transition to hypercapnia (1.25 ± 0.14) was not significantly different from control (1.21 ± 0.14); however gill burst duration during the transition from hypercapnia (1.43 ± 0.20) and the final control (1.28 ± 0.13) were significantly greater than control gill burst duration. Interburst interval was significantly increased in late developmental stage tadpoles during the transition to hypercapnia (0.65 ± 0.25), hypercapnic acidosis (0.79 ± 0.29), and the transition from hypercapnia (0.65 ± 0.25) when compared to control (0.58 ± 0.22).

Lung Respiratory Variables

Lung activity was highly variable between animals and some early developmental stage animals did not exhibit lung bursting activity during the initial control period making it difficult to compare variables such as cycle length and IBI, as at least two events are required to calculate. On the other hand, all late developmental stage preparations exhibited the expected low frequency, high amplitude fictive lung bursting pattern. Therefore, the lung burst-related variables were examined only in the late developmental stage animals (Table 1).

Lung burst frequency (min^{-1}) was significantly increased during the transition to hypercapnia (1.06 ± 0.30) when compared to control (0.29 ± 0.12). The lung burst cycle was significantly increased during the transition to hypercapnia (79.97 ± 25.88), the transition back to control (60.32 ± 31.80) when compared to the initial control lung burst cycle (8.15 ± 5.39). Lung burst duration (sec) during control bath pH (0.57 ± 0.19) was significantly less than lung burst duration during the transition to hypercapnic acidosis (1.21 ± 0.12) and the transition back to control aCSF (1.19 ± 0.12). Lung burst duration during hypercapnic acidosis (0.79 ± 0.14) and final control (0.79 ± 0.17) was not significantly different from any of the experimental conditions. Integrated

lung burst amplitude measured in arbitrary units during transition to hypercapnic acidosis (0.45 ± 0.05) and transition back to the final control (0.50 ± 0.05) were significantly increased when compared to lung burst amplitude during control aCSF (0.19 ± 0.07). Lung burst amplitudes during hypercapnic acidosis (0.31 ± 0.05) and during the final control period (0.36 ± 0.08) were not significantly different from the initial experimental conditions.

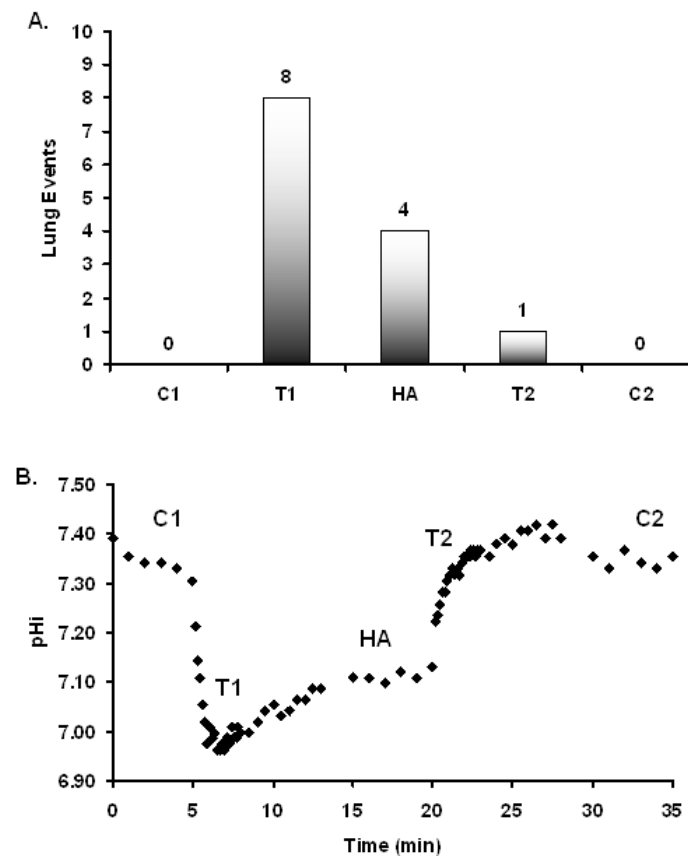
Pearson Product Moment Correlations were performed on respiratory variables and absolute pHi unit change to determine whether there was a quantitative relationship between intracellular pH and the respiratory motor output. A significant ($P < 0.05$) negative correlation (-0.706) was obtained when comparing absolute changes in pHi from cells located in chemosensitive regions of the tadpole brainstem and lung frequency (Table 2). There was no correlation between changes in pHi and respiratory variables in cells located in non-chemosensitive regions. An example of a preparation that exhibited a negative correlation between pHi and lung activity is shown in Fig. (4).

DISCUSSION

Two CO_2 chemosensitive regions have been identified in the tadpole brainstem [31-32]: one is rostral on the ventral surface of the brainstem at the level of CN V, and the other is more caudal, but also on the ventral surface of the brainstem at the level of CNs IX and X. In mammalian preparations, neurons in brain slices from adult animals regulate pHi poorly during hypercapnia whether they possess chemosensory activity or not [6, 33-34]. When the PCO_2 rises, pHi falls abruptly, remains low throughout the hypercapnic exposure (typically 20-40 minutes), and returns to the control level once the hypercapnic stimulus is removed. Neurons in brain slices from neonatal animals, on the other hand, regu-

Table 2. Pearson Product Moment Correlations for Lung Respiratory Variables and Absolute pHi Unit Change in Non-Chemosensitive and Chemosensitive Regions of the Tadpole Brainstem

| | Non- Chemosensitive Region | | Chemosensitive Region | |
|-----------|----------------------------|---------|-------------------------|---------------|
| | Correlation Coefficient | P Value | Correlation Coefficient | P Value |
| Frequency | 0.187 | 0.66 | -0.706 | 0.02 * |
| Cycle | -0.090 | 0.83 | 0.030 | 0.93 |
| Duration | 0.078 | 0.85 | 0.443 | 0.20 |
| IBI | -0.089 | 0.83 | 0.034 | 0.93 |
| Amplitude | 0.018 | 0.97 | 0.193 | 0.59 |

**Fig. (4).** Lung events expressed as a function of experimental condition (panel A) and simultaneous measurements of pHi in a single cell located in a chemosensitive region of the tadpole brainstem (panel B). Note: drops in pHi correspond to an increase in the number of lung events observed.

late pHi well during hypercapnia if they are non-chemosensory. The pHi in these neurons rises toward the control value during hypercapnia, and there is an alkaline overshoot when hypercapnia is removed as a result of the pHi regulatory processes active during hypercapnia. However, neurons in neonatal brain slices regulate pHi poorly (exactly like adult neurons) if they are in chemosensory nuclei [6,34]. All of these neurons, regardless of location and age of the animal, seem to regulate pHi well if pHe does not decrease during the acidic stress (e.g., isohydric hypercapnia). Thus, neurons possess pHi regulatory mechanisms, but a simultaneous decline in pHi and pHe seems to inhibit pHi

regulation in many neurons. Therefore, we asked whether pHi regulation differed among chemosensory and non-chemosensory sites in the tadpole brainstem. We incubated the *in vitro* tadpole brainstem in 40 μ M of the pH sensitive dye BCECF-AM, washed the extracellular dye away and then used glass suction electrodes to obtain whole nerve recordings of respiratory activity while we simultaneously measured pH using BCECF.

We performed simultaneous recordings of spontaneous respiratory motor output and pHi from neurons located in known chemosensitive and non-chemosensitive regions in

the brainstem of *Lithobatesbebianus*, an animal model well-suited to examine the neural development of respiration. Our combination of electrophysiology and fluorescence microscopy represents a novel approach to characterize central CO₂ chemoreceptors in the *in vitro* tadpole brainstem and has resulted in several significant findings: 1) there are significant differences in pHi both during normocapnia and during hypercapnia between neurons located in non-chemoreceptor and chemoreceptor regions, 2) neurons located in central respiratory chemoreceptor regions demonstrate pHi recovery when only pHi is reduced and pHe is held constant, and 3) we report direct correlation between changes in pHi and respiratory motor activity unique to neurons located in chemosensory regions in a vertebrate model of respiratory control.

When exposed to hypercapnic acidosis, there was a significant difference in the ability of cells located in both chemosensitive or non-chemosensitive regions to regulate pHi, indicating the potential for the presence of different ion transport mechanisms in cells located in chemosensitive and non-chemosensitive regions. If chemosensitive cells are to adequately monitor pH changes and convey these changes in pHi in the form of changes in firing rate, chemosensitive cells should remain relatively acidic when exposed to an acidic environment, i.e., a drop in *both* pHo and pHi. Studies in other animal preparations using pH-sensitive probes have also identified differences in the pHi regulatory processes of cells located in chemosensitive and non-chemosensitive regions [34-35]. In addition, using BCECF in tadpole brainstem neurons to record pHi optically does not disrupt respiratory rhythmicity or central respiratory chemoreception [36-38]. The pHi regulatory responses to hypercapnic acidosis reported in this study are consistent with those reported in the snail [39] and rat [6,34,35], indicating the evolutionary conservation of pHi regulatory mechanisms, although the persistence of pHi regulation in non-chemosensory cells, as seen in all tadpole developmental stages, is observed only in preparations from neonatal mammals. We observed a higher percentage of cells in non-chemosensitive regions that exhibit pHi regulation during hypercapnia (76%) when compared to the cells in chemosensitive regions (47%). Our data indicate that nearly half of the cells in chemosensitive regions regulate during hypercapnia (47%) compared to those cells in chemosensitive regions that do not regulate pHi during hypercapnic acidosis (53%); the percentage of cells exhibiting pHi regulation in the chemosensitive area in the tadpole reported in this study is similar to the percentage of neurons in the dorsal medulla of the rat (slices) that responded to hypercapnia (50%) [40]. The percentage of neurons which respond to hypercapnia in mammals varies from approximately 20% in raphe neurons [41], to up to 80% of neurons located in the locus coeruleus [42]. It is possible that the tadpole also exhibits a developmental increase in the number of cells responding to hypercapnia as reported in rats [43] and in pre-term human infants [44]

The ammonia prepulse is a technique used to elicit changes in pHi at a constant pHo. The use of the ammonia prepulse technique in this study decreased pHi to a similar extent to the decreases in pHi achieved by hypercapnic acidosis. More importantly, the response of the cells tested with the ammonia prepulse indicated that cells which demonstrate

no pHi regulation during HA, a condition in which both pHo and pHi decrease, do have the ability to regulate pHi when only pHi drops. Together, these data suggest that the signal that initiates pHi regulation is strongly linked to both pHo and pHi. The complement of ion transporters responsible for pHi regulation in the tadpole appear to be similar to those described in mammals. Initial studies in our lab demonstrated an adverse effect of bath applied NH₄Cl on whole nerve respiratory activity; however, the disruption of respiration is not surprising, as the NH₄Cl was bath applied and had the ability to alter pHi in all brainstem cells. This adverse effect has been demonstrated in other preparations [1]. Therefore other methods of focal intracellular acidification which do not disrupt central respiratory rhythmicity and chemoreception, such as uncaging H⁺ with ultraviolet light [38], should prove beneficial in further describing the correlation between respiratory motor output and pHi.

We recently adapted a technique to induce focal decreases in pHi alone while maintaining pHo to the tadpole brainstem preparation [38]. We bath applied the H⁺ donor, nitrobenzaldehyde, to the tadpole brainstem and used flash photolysis to decrease only pHi to values similar to those observed with hypercapnia. The "uncaging" of H⁺ using ultraviolet light induced decreases in pHi without disruption of respiratory rhythmicity. In addition, these data indicate significant pHi regulation following decreases in pHi alone similar to the rate of pHi regulation observed following the ammonium chloride prepulse technique reported in this study [35]. It is important to note that the lack of pHi regulation alone is not sufficient to identify a cell as a chemoreceptor, as some neurons that exhibit decreases in pHi and show no regulation did not show concomitant increases in firing rate [34]. Therefore, future whole cell recording confirming sustained intracellular acidification and a change in firing rate in particular neurons will be necessary.

Whole nerve respiratory activity was measured throughout hypercapnic acidosis, a condition where both pHo and pHi decrease. Respiratory variables were measured during five experimental conditions; control (C1), transition to hypercapnic acidosis (T1), hypercapnic acidosis (HA), transition back to control (T2), and post control (C2). It has been well documented that there is a developmental component to fictive tadpole ventilation in response of CO₂ [31, 23]. Therefore, a subset of animals between the stages of 3 - 9 (n = 10) and 11 - 20 (n = 8) were used to describe the ontogeny of whole nerve respiratory activity through hypercapnic acidosis and return to control bath pH.

Significant changes in the gill and lung burst timing components of cycle, duration, and IBI in response to exposure to hypercapnia were observed only in late developmental stage tadpoles, similar to findings by Taylor et al. [31] and Torgerson et al. [23]. The significant effects of hypercapnia on gill burst activities were limited to timing components, as we observed no significant changes in gill burst amplitude in response to hypercapnia in either the early or late developmental stage tadpoles. The lung burst responses to hypercapnia included both the timing components of frequency, cycle, duration, and IBI, but also included a significant increase in the lung burst amplitude. These respiratory responses to hypercapnia are similar to previously reported

gill and lung burst responses to hypercapnia in the tadpole brainstem preparation [31, 23]. Our data support previous studies and provide new important information regarding the transition values *to* and *from* hypercapnia, periods where dynamic changes in both respiratory motor output and chemoreceptor pHi have been presumed to occur. Moreover, these findings support the contention that respiratory central chemosensory function emerges in mid to late stage tadpoles [23]. Despite equivalent reductions in pHi during hypercapnia, the early stage tadpoles were unresponsive to hypercapnia, whereas both the gill and lung bursting patterns were modified by hypercapnia in the later stage tadpoles.

In the present study there was a significant correlation between a drop in pHi in cells located in chemosensitive regions and an increase in lung burst frequency. The correlation between decreases in pHi of cells located in non-chemosensitive regions and increases in lung frequency was not observed. Because the entire brainstem was exposed to hypercapnia, it is possible that neurons other than those located in chemosensitive areas were responsible for driving ventilation. We are not claiming that the neurons located in documented chemosensitive regions that demonstrated a sustained decrease in pHi with hypercapnia are driving ventilation. Rather, these neurons in known chemosensitive regions possess one of the primary properties of central respiratory chemoreceptors, namely a maintained acidification in response to hypercapnic acidosis [42]. Although this study did not aim to record the neuronal activities of neurons, we provide evidence of two distinct populations of neurons with respect to their pHi profiles during hypercapnia; 1) neurons located in known non-chemosensitive areas that demonstrates regulation of pHi and no correlation to respiratory motor output, and 2) neurons located in previously defined chemosensitive regions that demonstrate a relative lack of regulation of pHi during hypercapnia and an inverse correlation between pHi and lung burst activities. The finding of a correlation between decreases in pHi and increases in lung frequency is novel and supports the hypothesis that decreases in pHi in central respiratory chemoreceptors are the proximate stimulus driving the increase in ventilation associated with hypercapnia [42].

KNOWLEDGMENT

This research was funded by the National Institutes of Health National Center for Research Resources Research Centers in Minority Institutions (RCMI) Program grant 5G12 RR013646-08 awarded to MJG, and the National Institutes of Health National Institute of General Medical Sciences Minority Access to Research Careers (MARC) grant GM60655 awarded to DAZ.

REFERENCES

- Filosa JA, Dean JB, Putnam RW. Role of intracellular and extracellular pH in the chemosensitive response of rat locus coeruleus neurons. *J Physiol* 2002; 541: 493-509.
- Putnam RW. Intracellular pH regulation of neurons in chemosensitive and nonchemosensitive areas of brain slices. *Resp Physiol* 2001; 129: 37-56.
- Richerson GB. Serotonergic neurons as carbon dioxide sensors that maintain pH homeostasis. *Nat Rev Neuro*. 2004; 5: 449-61.
- Nattie EE, Li A. Central chemoreception in the region of the ventral respiratory group in the rat. *J Appl Physiol* 1996; 81: 1987-95.
- Guyenet PG, Bayliss DA, Stornetta RL, Fortuna ML, Abbott SB, Depuy SD. Retrotrapezoid nucleus, respiratory chemosensitivity and breathing automaticity. *Respir Physiol Neurobiol* 2009; 168(1-2): 59-68.
- Ritucci NA, Chambers-Kersh L, Dean JB, Putnam RW. Intracellular pH regulation in neurons from chemosensitive and nonchemosensitive areas of the medulla. *Am J Physiol Regul Integr Comp Physiol* 1998; 275: 1152-63.
- Ramanantsoa N, Hirsch MR, Thoby-Brisson M, et al. Breathing without CO₂ sensitivity in conditional Phox2b mutants. *J Neurosci* 2011; 31(36): 12880-8.
- Ray RS, Corcoran AE, Brust RD, et al. Impaired respiratory and body temperature control upon acute serotonergic neuron inhibition. *Science* 2011; 333: 637-42.
- Zhang X, Su J, Cui N, Gai H, Wu Z, Jiang C. The disruption of central CO₂ chemosensitivity in a mouse model of Rett syndrome. *Am J Physiol Cell Physiol* 2011; 301(3): C729-38.
- Brockhaus J, Ballanyi K, Smith JC, Richter DW. Microenvironment of respiratory neurons in the *in vitro* brainstem spinal cord of neonatal rats. *J Physiol* 1993; 462: 421-45.
- Dutschmann M, Wilson RJ, Paton JF. Respiratory activity in neonatal rats. *Auton Neurosci* 2000; 84: 19-29.
- Morin-Surun MP, Denavit-Saubie M. Rhythmic discharges in the perfused isolated brainstem preparation of adult guinea pig. *Neurosci Lett* 1989; 101: 57-61.
- Paton JF. Functionally intact *in vitro* preparation generating respiratory activity in neonatal and mature mammals. *Pflügers Arch* 1993; 428: 250-60.
- Richter DW, Spyer KM. Studying rhythmogenesis of breathing: comparison of *in vivo* and *in vitro* models. *TRENDS Neurosci* 2001; 464-72.
- Smith JC. Neural mechanisms generating respiratory pattern in mammalian brain stem-spinal cord *in vitro*. I. Spatiotemporal patterns of motor and medullary neuron activity. *J Neurophysiol* 1990; 64: 1149-69.
- Johnson SM, Turner SM, Huxtable AG, et al. Isolated *in vitro* brainstem-spinal cord preparations remain important tools in respiratory neurobiology. *Resp Physiol Neurobiol* 2012; 180: 1-7.
- Abdala APL, Rybak IA, Smith JC, et al. Multiple pontomedullary mechanisms of respiratory rhythmogenesis. *Respir Physiol* 2009; 19-25.
- St. John WM. Medullary regions for neurogenesis of gasping: no eud vital or no euds vitals? *J Appl Physiol* 1996; 81: 1865-77.
- Wang W, Fung ML, Darnall RA, St John WM. Characterizations and comparisons of eupnoea and gasping in neonatal rats. *J Physiol* 1996; 490: 277-92.
- Smith JC, Abdala APLH, Koizumi H, Rybak IA, Paton JFR. Spatial and functional architecture of the mammalian brain stem respiratory network: A hierarchy of three oscillatory mechanisms. *J Neurophysiol* 2007; 98: 3370-87.
- Torgerson CS, Gdovin MJ, Kogo N, Remmers JE. Depth profiles of pH and PO₂ in the *in vitro* brainstem preparation of the tadpole *Rana catesbeiana*. *Resp Physiol* 1997; 108: 205-213.
- Torgerson CS, Gdovin MJ, Remmers JE. Location of central chemoreceptors in the developing tadpole. *Am J Physiol Regul Integr Comp Physiol* 2001; 280: 921-928.
- Torgerson CS, Gdovin MJ, Remmers JE. The ontogeny of central chemoreception during fictive gill and lung ventilation of an *in vitro* brainstem preparation of *Rana catesbeiana*. *J Exp Biol* 1997; 299: 2063-2072.
- Taylor AC, Kollros J. Stages in the normal development of *Rana pipiens* larvae. *Anat Rec* 94: 7-24, 1946.
- Boens N, Qin W, Basaric N, Orte A, Talavera EM, Alvarez-Pez JM. Photophysics of the fluorescent pH indicator BCECF. *J Phys Chem A* 2006; 110: 9334-9343.
- Rotman B, Papermaster BW. Membrane properties of living mammalian cells as studied by enzymatic hydrolysis of fluorogenic esters. *Proc Nat Acad Sci* 1966; 55: 134-141.
- Thomas JA, Buchsbaum RN, Zimniak A, Racker E. Intracellular pH measurements in Ehrlich ascites tumor cells utilizing spectroscopic probes generated *in situ*. *Biochem* 1979; 81: 2210-8.
- Tsien RY. A non-disruptive technique for loading calcium buffers and indicators into cells. *Nature* 1981; 290: 527-8.
- Gdovin MJ, Torgerson CS, Remmers JE. Neurorespiratory pattern of gill and lung ventilation in the decerebrate spontaneously breathing tadpole. *Resp Physiol* 1998; 113: 135-46.

- [30] Gdovin MJ, Torgerson CS, Remmers JE. Gill and lung respiratory pattern generation in the *in vitro* brainstem preparation of developing *Rana catesbeiana*. *J Comp Biochem Physiol* 124: 275-286: 1999.
- [31] Taylor B, Harris M, Leiter JC, Gdovin MJ. Ontogeny of central CO₂ chemoreception: chemosensitivity in the ventral medulla of developing bullfrogs. *Amer J Physiol Regul Integr Comp Physiol* 2003; 285(6): 1461-72.
- [32] Taylor B, Croll AD, Drucker ML, Wilson AL. Developmental exposure to ethanol or nicotine inhibits the hypercapnic ventilatory response in tadpoles. *Resp Physiol Neurobiol* 2008; 160: 83-90.
- [33] Richerson GB. Response to CO₂ of neurons in the rostral ventral medulla *in vitro*. *J Neurophysiol* 1995; 73: 933-44.
- [34] Ritucci NA, Erlichman JS, Leiter JC, Putnam RW. Response of membrane potential (Vm) and intracellular pH (pHi) to hypercapnia in neurons and astrocytes from rat retrotrapezoid nucleus (RTN). *Am J Physiol Regul Integr Comp Physiol* 2005; 289: 851-61.
- [35] Nottingham S, Leiter JC, Wages P, Buhay S, Erlichman JS. Developmental changes in intracellular pH regulation in medullary neurons of the rat. *Am J Physiol Regul Integr Comp Physiol* 2001; 281: 1940-51.
- [36] Gdovin MJ, Zamora DA, MaruthaRavindran CR, Costanzo M, Leiter JC. Employing a pH sensitive fluorophore to measure intracellular pH in the *in vitro* brainstem preparation of *Rana catesbeiana*. *Open Zool J* 2009; 2: 117-23.
- [37] Gdovin MJ, Zamora DA, MaruthaRavindran CR, Leiter JC. Optical recording of intracellular pH in respiratory chemoreceptors. *Ethn Dis* 2010; 20: (S1) 33-8.
- [38] Ravindran MCR, Bayne JN, Bravo SC, *et al*. Intracellular acidosis and pH regulation in central respiratory chemoreceptors. *J Health Care Poor Underserv* 2011; 22(4): 174-86.
- [39] Goldstein J, Mok JM, Simon CM, Leiter JC. Intracellular pH regulation in neurons from chemosensitive and nonchemosensitive regions of *Helix aspersa*. *Am J Physiol Regul Integr Comp Physiol* 2000; 279: 414- 23.
- [40] Huang RQ, Erlichman JS, and Dean JB. Cell-cell coupling between CO₂-excited neurons in the dorsal medulla oblongata. *Neuroscience* 1997; 80: 41-57.
- [41] Wang W, Pizzonia JH, Richerson GB. Chemosensitivity of rat medullary raphe neurones in primary tissue culture. *J Physiol* 1998; 511: 433-50.
- [42] Putnam RW. Role of pH in Cellular CO₂ Chemosensitivity. *J Appl Physiol* 2010; 108: 1796-1802.
- [43] Wang W and Richerson GB. Development of chemosensitivity of rat medullary raphe neurons. *Neuroscience* 1999; 90: 1001-11.
- [44] Krauss AN, Klain DB, Waldman S, Auld PAM. Ventilatory response to carbon dioxide in newborn infants. *Pediatr Res* 1975; 9: 46-50.

Received: August 17, 2013

Revised: August 20, 2013

Accepted: August 21, 2013

© Zamora *et al.*; Licensee Bentham Open.This is an open access article licensed under the terms of the Creative Commons Attribution Non-Commercial License (<http://creativecommons.org/licenses/by-nc/3.0/>) which permits unrestricted, non-commercial use, distribution and reproduction in any medium, provided the work is properly cited.